

Initial Laboratory-Scale Melter Test Results for Combined Fission Product Waste

Advanced Fuel Cycle Initiative

***Prepared for
U.S. Department of Energy
Waste Forms Campaign
B.J. Riley, J.V. Crum, W.C. Buchmiller,
B. T. Rieck, M. J. Schweiger,
J. D. Vienna***

September 21, 2009

AFCI-WAST-PMO-MI-DV-2009-000184



DISCLAIMER

This information was prepared as an account of work sponsored by an agency of the U.S. Government. Neither the U.S. Government nor any agency thereof, nor any of their employees, makes any warranty, expressed or implied, or assumes any legal liability or responsibility for the accuracy, completeness, or usefulness, of any information, apparatus, product, or process disclosed, or represents that its use would not infringe privately owned rights. References herein to any specific commercial product, process, or service by trade name, trade mark, manufacturer, or otherwise, does not necessarily constitute or imply its endorsement, recommendation, or favoring by the U.S. Government or any agency thereof. The views and opinions of authors expressed herein do not necessarily state or reflect those of the U.S. Government or any agency thereof.

SUMMARY

Pacific Northwest National Laboratory (PNNL) and Savannah River National Laboratory performed a joint study to develop acceptable glasses for the combined alkali and alkaline-earth fission products (CS) + lanthanide fission products (LN) + transition metal fission products (TM) waste streams and CS + LN combined waste streams. Glass CSLNTM-C-2.5 was selected as the baseline glass for the CS + LN + TM waste stream as it had the highest MoO₃-loaded glass that did not crystallize during slow cooling and it had properties within acceptable tolerances for glass processing and waste form performance (Crum et al., 2009).

To obtain an initial understanding on the processability of this selected glass composition, initial small-scale melter tests were performed. This report summarizes the melter feed processing in a 3"-diameter laboratory-scale melter at PNNL as well as techniques that could be employed to improve the efficiency of vitrifying such a waste stream. Two experiments were run (including a shakedown test) in the melter with the same feed, representative of the actual waste stream. Reaction vessel and off-gas line solid condensates were analyzed to perform a mass-balance of the most volatile components - Cs and Mo. The analysis of the condensates showed that volatile components (i.e., Cs, Mo) evolved during the melting process at reasonable concentrations. From these studies, it is apparent that a recuperator for the volatile compounds should be considered.

CONTENTS

SUMMARY	iii
ACRONYMS AND ABBREVIATIONS	viii
1. Introduction	1
2. Experimental.....	2
2.1 Feed Composition and Preparation	2
2.2 Thermochemical Denitration	5
2.3 Melter Preparation and Operation.....	5
2.4 Melter Run No. 1 (LSM-R1).....	9
2.5 Melter Run No. 1 (LSM-R2).....	11
2.6 X-ray Diffraction.....	11
2.7 Scanning Electron Microscopy	11
3. Results AND Discussion	11
3.1 Analysis of Denitration Solution and Precipitates	11
3.2 General Results from Melter Runs.....	12
3.3 LSM-R1 Results.....	13
3.4 LSM-R2 Results.....	13
3.5 Off-Gas Condensate Solids Analysis	15
4. Conclusions and Future Work.....	21
5. Acknowledgements	22
6. References	22

FIGURES

Figure 1. Acid distillation and reduction apparatus.	4
Figure 2. Schematic of crucibles used in experiments.....	6
Figure 3. Schematic of PNNL laboratory-scale melter used in this study.	7
Figure 4. Profiling the peristaltic pump for flow rate (mL/min) per RPM on the pump. <i>NOTE: the trend-line was forced through zero.</i>	7
Figure 5. Furnace profiling. (A) The temperature measured by three thermocouples at a distance, <i>Submersion into furnace</i> , which was the distance (in inches) from the thermocouple to the top of the hot zone inside the furnace. (B) The summary of average temperature (of all thermocouples) of the different distances with standard deviation where more than	

one measurement was taken at a given distance. (C) Schematic of the procedure used and how the scale, <i>Submersion into furnace</i> , relates to the setup used.	9
Figure 6. Pictures of LSM-R1 at different stages during assembly of the resultant vitrified feed.....	13
Figure 7. Optical micrographs of the glass produced from LSM-R2. (A) Shows the glass out of the crucible. (B) Shows the glass that stuck to the bottom of the crucible and the zirconia stage.	14
Figure 8. Comparison of targeted and EDS (measured) compositions for vitrified feed from LSM-R2.	15
Figure 9. Regions where condensates were observed (#1–#5) and the scrubber solution (#6) where soluble salts were expected. <i>NOTE: this is a cut-out from Figure 3.</i>	16
Figure 10. XRD results for the condensate inside the quartz tube inlet from LSM-R1 (Figure 9, #1).....	17
Figure 11. XRD results for the condensate inside the quartz tube off-gas line from LSM-R1 (Figure 9, #2).	18
Figure 12. XRD results for the condensate inside the scrubber feed tube from LSM-R2 (Figure 9, #3).....	18
Figure 13. XRD results for the condensate inside the Teflon from LSM-R2 (Figure 9, #4).	19
Figure 14. (A) SEM on the condensates collected off the inside of the inlet port on the quartz crucible (Figure 9, #1) at 500× and (B) SEM on the condensates from the off-gas line on the quartz crucible (Figure 9, #2) at 500×.	19
Figure 15. (A) SEM micrograph (1.5 k×) of scrubber feed line condensate collected at end of LSM-R2 (#3, Figure 9), (B) SEM micrograph (500×) of the condensate inside of the Teflon tube from LSM-R2 (#4, Figure 9), and (C) SEM micrograph (750×) of Teflon tube condensate (#4, Figure 9). The boxes and labels in (C) show the locations of small area EDS analysis that was performed.	20
Figure 16. Quantities (in mass%) of each additive (except for SiO ₂) in condensates #1–#4 (see Figure 9).	21

TABLES

Table 1. Target compositions and properties for CSLNTM-C-2.5 (Crum et al., 2009).	1
Table 2. Compositions of the TRUEX raffinate and the TALSPEAK product (strip) (Benker et al., 2008).	2
Table 3. Data for waste stream additives for 10 L volume (V) of feed at a final acid concentration of 2.915 M HNO ₃	2
Table 4. Composition of melter feed based on 100 g of oxide made. The feed additives are listed above the double line and the glass formers below it.	4
Table 5. Batch sheet for LSM-R1.	10
Table 6. Ion chromatography of solution aliquots.	12
Table 7. SEM/EDS on thermochemical reduction precipitate before (Unrinsed) and after rinsing (DIW-Rinsed) with DIW to remove compounds soluble in neutral pH.	12

Table 8. General parameters for LSM runs.....	12
Table 9. Differences between the targeted and measured (EDS) compositions for LSM-R2 vitrified feed. “% Diff.” is the % difference between the measured and targeted values.....	14
Table 10. Quantities (g) of condensates (#1-#4), precipitates (#5), or solutions (#6) collected and estimated for each region from Figure 9. <i>NOTE: the value for #6 is in mass (g) of the liquid collected from the scrubber solution and since the amount of dissolved materials were never quantified it was not included in the “Totals” value.</i>	16
Table 11. EDS results (in mass%) from LSM-R1 crucible condensates listed by element. “Inlet” and “Off-Gas” correspond to #1 and #2, respectively from Figure 9.....	20
Table 12. EDS results (in mass%) from LSM-R2 condensates listed as element.....	21

ACRONYMS AND ABBREVIATIONS

AFCI	Advanced Fuel Cycle Initiative
CS	alkaline / alkaline earth fission products
DIW	deionized water
DOE	United States Department of Energy
EDS	energy dispersive spectroscopy
FY	fiscal year(s)
LN	lanthanide fission products
NE	Nuclear Energy
PNNL	Pacific Northwest National Laboratory
LSM	laboratory scale melter
SEM	scanning electron microscope (microscopy)
SRNL	Savannah River National Laboratory
T_g	glass transition temperature
T_L	liquidus temperature
T_M	glass melting temperature
TALSPEAK	trivalent actinide-lanthanide separation by phosphorous reagent extraction from aqueous complexes
TM	transition metal fission products
TRUEX	transuranics extraction process
UREX	uranium extraction process
XRD	X-ray diffraction

ADVANCED FUEL CYCLE INITIATIVE

GLASS PROCESSING

1. INTRODUCTION

Pacific Northwest National Laboratory (PNNL) and Savannah River National Laboratory (SRNL) performed a joint study to develop acceptable glasses for the combined alkali and alkaline-earth fission products (CS) plus lanthanide fission products (LN) plus transition metal fission products (TM) waste streams (Option 1) and CS + LN combined waste streams (Option 2) generated by a representative uranium extraction group of aqueous fuel separations processes (UREX+) being developed by the Advanced Fuel Cycle Initiative (AFCI). Discussion of the waste compositions used and the glass formulations is reported by Crum et al. (2009).

Glass “CSLNTM-C-2.5” was selected as the baseline glass among the five glasses fabricated and tested for Option 1 (high MoO₃, 1-3.5 mass%), for the glass limited by high MoO₃ at 2.5 mass%, where phase separation was not observed during melting or characterization. This glass was the highest MoO₃-loaded glass that did not crystallize upon slow cooling, and the measured glass properties (i.e., T_L , viscosity, electrical conductivity, and measured release rates of the quenched and slow cooled glass) were all well within the acceptable range for glass processing and waste form performance. Table 1 (taken from Crum et al., 2009) lists the target composition and properties of CSLNTM-C-2.5.

In this study, CSLNTM-C-2.5 was formulated into a melter feed (minor components and noble metals were removed) and was processed in the PNNL laboratory-scale melter (LSM). The resultant glass and off-gas condensates were analyzed. The results are presented in this report.

Table 1. Target compositions and properties for CSLNTM-C-2.5 (Crum et al., 2009).

Property	CSLNTM-C-2.5	Key Components	Mass%
Quenched crystallinity, mass%	Trace RuO ₂	Al ₂ O ₃	5.95
Slow cooled crystallinity, mass%	Trace RuO ₂	B ₂ O ₃	5.00
Optical T_L , °C	1017	SiO ₂	53.03
XRD T_L , °C	1030	Cs ₂ O	1.84
Primary crystalline phase	Ca ₂ Nd ₈ Si ₆ O ₂₆	BaO	1.41
Quenched PCT B, g/L	0.21	SrO	0.63
Slow cooled PCT B, g/L	0.19	Ln ₂ O ₃	8.58
Density, g/cm ³	2.78	MoO ₃	2.50
T_g , °C	515	ZrO ₂	1.91
T_M , °C	1233		
A ^(a)	-8.68		
B ^(a)	15505		
ϵ at T_M , S/m	20.53		
C ^(b)	8.42		
D ^(b)	-8124	Other ^(c)	19.15

(a) $\ln[\eta, \text{Pa}\cdot\text{s}] = A + B/T$

(b) $\ln[\epsilon, \text{S/m}] = C + D/T$

(c) Sum of other components not listed above

2. EXPERIMENTAL

2.1 Feed Composition and Preparation

The waste simulant was based on a combination of the TRUEX raffinate and the TALSPEAK product (strip) for 24 GWd/MTIHM, or gigawatt day per metric ton initial heavy metal, with ~33 year decay time as presented in the CETE-1 Report (Benker et al., 2008). The compositions of these individual streams as well as a combined stream are found in Table 2.

Table 2. Compositions of the TRUEX raffinate and the TALSPEAK product (strip) (Benker et al., 2008).

Process:	TRUEX	TALSPEAK	Combined	Unit
Stream:	raffinate	product (strip)		
Volume	65.7	35.4	101.1	L
H ⁺	170.82	123.9	294.72	moles
Actinides	4.11E-02	4.78E-02	8.89E-02	g
Lanthanides	0.539	21.2	21.8	g
Alkali	4.98	9.41E-04	4.98	g
Alkaline Earth	6.60	6.24E-02	6.67	g
Transition Metals	10.65	1.34E-01	10.8	g
Noble Metals	4.41E-01	1.51E-03	4.42E-01	g
Total Fuel	23.3	21.5	44.7	g

For the actual melter feed, Nd was substituted for the actinides on a mole basis (i.e., U, Pu, Np, Am, and Cm) and Tc, Ru, and Pd were omitted. Using the element amounts listed in Table 2 and a total solution volume of 101.1 L, the molarity of each element in the combined solution was calculated (see Table 3). Similarly, the molarity of free acid (H⁺) of the combined solution was determined to be 2.915 M. A conversion factor between the molarity of the element in solution and the molarity of the HNO₃ was used to preserve the molar ratios between the elements and the H⁺ in the waste stream. The simulant components were added as nitrates according to the recipe in Table 3. The mass of each additive, $Mass_{Additive}$, was calculated using the following:

$$Mass_{Additive} = (M_{Element} / M_{HNO3}) * M_{HNO3} * MW_{Additive} * V \quad (1)$$

where $M_{Element}$ is the molarity of the element in solution, M_{HNO3} is the molarity of HNO₃, $MW_{Additive}$ is the molecular weight of the additive, and V is the desired total volume of feed.

Table 3. Data for waste stream additives for 10 L volume (V) of feed at a final acid concentration of 2.915 M HNO₃.

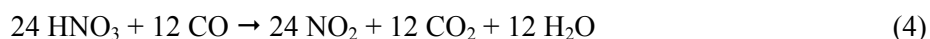
Element	Mol _{Element}	M _{Element} , mol/L	M _{Element} / M _{HNO3}	Additive	Mass _{Additive} , g
Ba	3.634E-02	3.595E-04	1.233E-04	Ba(NO ₃) ₂	0.9395
Ce	3.606E-02	3.567E-04	1.223E-04	Ce(NO ₃) ₃ *6H ₂ O	1.5487
Cs	3.299E-02	3.263E-04	1.119E-04	CsNO ₃	0.6360
Eu	1.645E-03	1.627E-05	5.582E-06	Eu(NO ₃) ₃ *6H ₂ O	0.0726
Gd	2.228E-03	2.203E-05	7.559E-06	Gd(NO ₃) ₃ *5H ₂ O	0.0955
La	1.966E-02	1.944E-04	6.670E-05	La(NO ₃) ₃ *6H ₂ O	0.8419
Mo	6.202E-02	6.135E-04	2.104E-04	MoO ₃	0.8830

Element	Mol _{Element}	M _{Element} , mol/L	M _{Element} / M _{HNO3}	Additive	Mass _{Additive} , g
Nd	6.479E-02	6.409E-04	2.198E-04	Nd(NO ₃) ₃ *6H ₂ O	2.8092
Pr	1.806E-02	1.786E-04	6.127E-05	Pr(NO ₃) ₃ *6H ₂ O	0.7770
Rb	6.932E-03	6.857E-05	2.352E-05	RbNO ₃	0.1011
Sm	1.020E-02	1.009E-04	3.462E-05	Sm(NO ₃) ₃ *6H ₂ O	0.4486
Sr	1.911E-02	1.890E-04	6.482E-05	Sr(NO ₃) ₂	0.3999
Y	9.172E-03	9.072E-05	3.112E-05	Y(NO ₃) ₃ *6H ₂ O	0.3475
Zr	4.144E-02	4.099E-04	1.406E-04	ZrO(NO ₃) ₂ *2H ₂ O	1.0954
				Total:	10.9960

According to Table 3, at 2.915 M HNO₃, 10 L of the combined TRUEX raffinate and the TALSPEAK product would include only ~11 g of solids, and hence it was determined that the solids would have to be significantly concentrated in the melter feed. Melter feed should be targeted between 300 and 1000 g of glass per liter of feed for efficient melting. If not, there would be a significant burden placed on the melter (and/or calciner) and off-gas system to treat the large quantities of acid and noxious gas given off during processing. Reducing the volume of the solvent prior to melting provides an opportunity to recover some of the nitric acid which could be recycled. Existing techniques are available to accomplish this, for example vacuum distillation and nitrate chemical reduction.

Nitric acid vacuum distillation is a simple, well demonstrated technology (see Smith et al., 1999, for example). Heating a HNO₃ solution to 63°C at moderate vacuum levels (i.e., 125 Torr) distills HNO₃ without significant decomposition. Through this process, water was removed first, and, once the concentration of the HNO₃ reached the azeotropic point (~16 M or ~70%), the HNO₃ was evolved.

Further removal of the HNO₃ could be done using a thermochemical denitration process (i.e., chemical reduction [see section 2.2, Thermochemical Denitration]). The reaction of sucrose (C₁₂H₂₂O₁₁) with HNO₃ would result in byproducts such as CO_x, NO_x, and H₂O as in reactions (2) through (5) (Bray, 1963):



According to these reactions, 12–48 moles of HNO₃ can be destroyed per mole of sucrose added. This was performed using a laboratory described by Smith et al. (1999) and shown schematically in Figure 1.

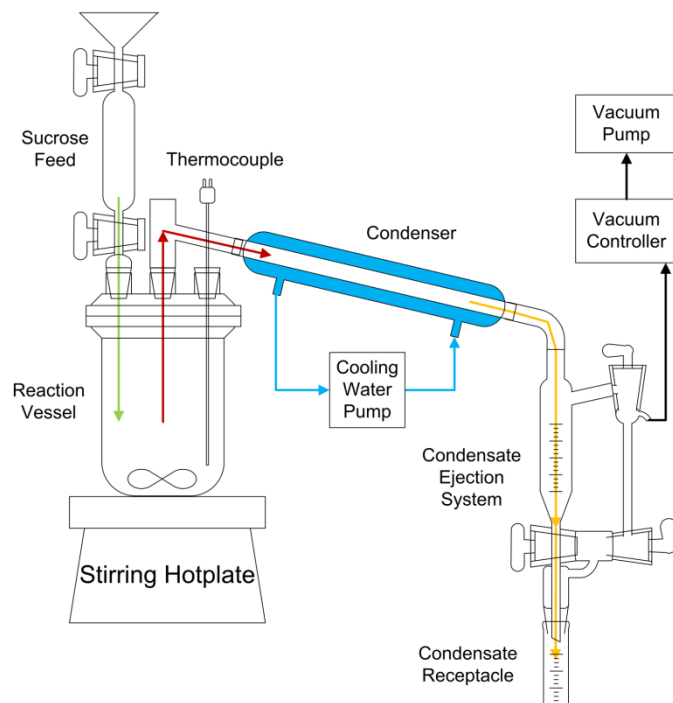


Figure 1. Acid distillation and reduction apparatus.

A lower nitrate melter feed simulant was fabricated based on the waste composition used to formulate CSLNTM-C-2.5 with the noble metals and minor components removed, as shown in Table 4.

Table 4. Composition of melter feed based on 100 g of oxide made. The feed additives are listed above the double line and the glass formers below it.

Oxide	Mass oxide, g (per 100 g)	Additive	Mass additive, g (per 100 g of oxide)
BaO	1.42	Ba(NO ₃) ₂	2.43
Ce ₂ O ₃	2.00	Ce(NO ₃) ₃ *6H ₂ O	5.30
Cs ₂ O	1.86	CsNO ₃	2.57
Eu ₂ O ₃	0.11	Eu(NO ₃) ₃ *6H ₂ O	0.28
Gd ₂ O ₃	0.10	Gd(NO ₃) ₃ *5H ₂ O	0.25
La ₂ O ₃	1.02	La(NO ₃) ₃ *6H ₂ O	2.71
MoO ₃	2.52	MoO ₃	2.52
Nd ₂ O ₃	3.38	Nd(NO ₃) ₃ *6H ₂ O	8.82
Pr ₂ O ₃	0.93	Pr(NO ₃) ₃ *6H ₂ O	2.47
Rb ₂ O	0.27	RbNO ₃	0.43
Sm ₂ O ₃	0.69	Sm(NO ₃) ₃ *6H ₂ O	1.77
SrO	0.63	Sr(NO ₃) ₂	1.29
Y ₂ O ₃	0.41	Y(NO ₃) ₃ *6H ₂ O	1.38
ZrO ₂	1.93	ZrO(NO ₃) ₂ *2H ₂ O	4.18
Al ₂ O ₃	6.00	Al ₂ O ₃	6.00
B ₂ O ₃	5.04	H ₃ BO ₃	8.96
CaO	7.06	CaCO ₃	12.60

Oxide	Mass oxide, g (per 100 g)	Additive	Mass additive, g (per 100 g of oxide)
Li ₂ O	4.05	Li ₂ CO ₃	10.01
Na ₂ O	7.06	Na ₂ CO ₃	12.08
SiO ₂	53.49	SiO ₂	53.49
	100.00		139.53

2.2 Thermochemical Denitration

A scoping test to demonstrate thermochemical denitration was performed by adding sucrose to the waste feed simulant. A 0.5 L solution of concentrated HNO₃ (15–17 M) with representative waste components dissolved into solution was heated in a 1 L beaker at 85°C. Over 0.5 hours, 4.42 g of sucrose was intermittently added to solution. The components were added in nitrate form as in Table 3, corrected for the adjusted volume and HNO₃ concentration using Equation (1). The solution turned from light yellow to a dark brown as the sucrose was added and a yellow plume of vapor evolved from the solution for 3 hours, resulting in a volume loss of ~150 mL. Heating was discontinued and while the solution remained overnight, ~50 mL of vapors slowly evolved, and a white precipitate was observed on the bottom of the beaker. Heating at 85°C was resumed for 6 hours until ~75 mL remained in the beaker with the white precipitate at the bottom.

The precipitate was collected from the bottom of the beaker, placed on a 0.45 μm filter, and then dried using vacuum filtration. A small aliquot of the filtrate was collected. The rest of the filtrate was then rinsed with deionized water (DIW) to remove any salts soluble at a more neutral pH. Dried powders of these two precipitates were placed on a scanning electron microscopy (SEM) stub using carbon tape and then were analyzed by SEM with energy dispersive spectroscopy (EDS) for composition.

Aliquots were removed from the beaker at the start of the test, the following morning prior to reheating, and at the end of the test when the solution was at temperature. These aliquots were analyzed using a Dionex 3000 ion chromatography system and an AS11-HC column. The eluent was 30 mM hydroxide. Calibration was performed a certified standard.

2.3 Melter Preparation and Operation

The melter assembly chosen for these experiments was the PNNL laboratory-scale melter (LSM). This melter is shown schematically in Figure 2 and Figure 3. The single-use fused quartz crucible melter bodies were 3 in. outer diameter (OD) and 10 in. tall with two smaller ports (3/4 in. OD) off the top extending 7 in. The vertical tube was used as the feed inlet and the slanted tube for off-gas collection. The wall thickness on the primary vessel was 2.6 mm and 3.3 mm on the inlet and off-gas tubes. The top and bottom of the primary vessel were tapered down using a glass-working lathe and a torch and therefore were variable in thickness.

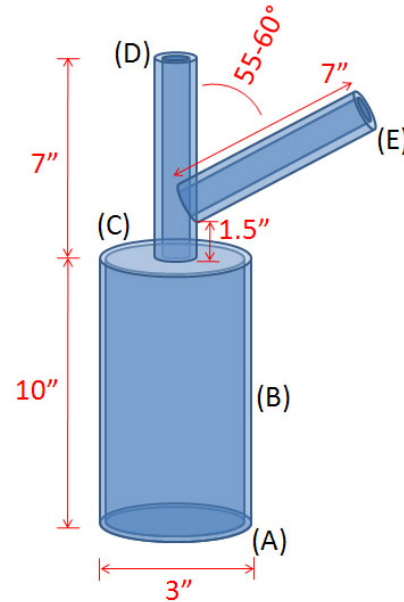


Figure 2. Schematic of crucibles used in experiments.

In previous LSM tests, these crucibles were supported with clamps and moved, into the hot zone of the furnace, as the melt layer height increased. A different approach was taken for these experiments. The crucible was anchored and remained stationary throughout the melting process. Instead, the furnace moved vertically (see Figure 3). This process was chosen to reduce stress on the quartz crucible and prevent a crucible failure. In this approach, the crucible was placed on top of a zirconia refractory cylinder, 3 in. OD (10 in. height), supported on a narrow, stationary table. A lift system supporting the furnace allowed it to be independently raised to surround the crucible. Granular alumina was placed between the bottom of the crucible and the top of the zirconia support cylinder to evenly displace the mass of the crucible on the support.

The feed line consisted of a flexible polyethylene tube connected to a 1/8 in. OD Inconel[®] 690 feed nozzle, with a 90-degree bend for insertion into the feed tube on the crucible and a small flare at the exit to help prevent feed build-up on the tip. The primary off-gas line consisted of high density Teflon tubing led to a wet scrubber. Following the scrubber, the off-gas was routed through a pair of condensers. The condensers and the scrubber were all cooled using a water chiller set at 10°C. The entire system was placed under a nominal vacuum of 7.5 Torr (4 in. water column) to help draw the off-gas through the scrubber and condensers. A stopcock located at the bottom of the condenser, in conjunction with the 3-way ball valve and air intake valve, was used to drain the condensed liquids.

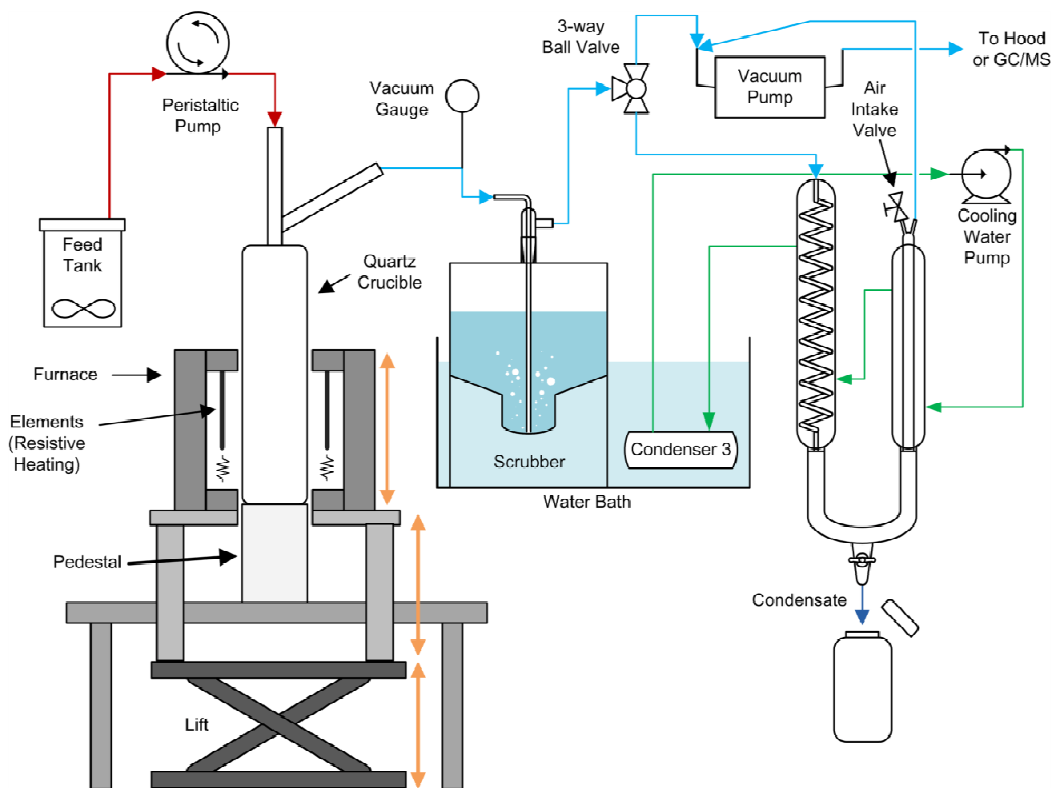


Figure 3. Schematic of PNNL laboratory-scale melter used in this study.

Once the melter was assembled, the furnace was run through a shakedown test to verify the feed system flow-rates per peristaltic pump settings, the heating capacity of the furnace, and the temperature profile of the hot zone at different crucible depths in the furnace. To calibrate the peristaltic pump, the RPM dial was set at a particular value, and DIW was flowed through the pump (with the pump nozzle in place) and the volume collected in a beaker on the receiving end. The rate (Figure 4) was then calculated using the volume recovered versus the elapsed time.

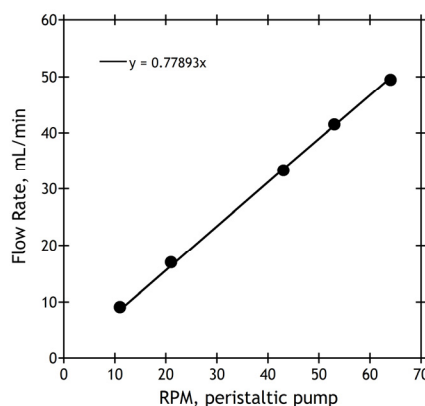


Figure 4. Profiling the peristaltic pump for flow rate (mL/min) per RPM on the pump. *NOTE: the trend-line was forced through zero.*

For profiling the furnace, three type K thermocouples were bundled and placed in the quartz reaction vessel. The thermocouples were spaced 2 in. apart, spanning a total of 4 in., with the bottom thermocouple resting on the bottom of the crucible. Starting from a fully lowered position, the furnace

was raised in 1-in. increments (with the crucible outside of the top of the furnace) and remained stationary at each position until thermal equilibrium was achieved (10-15 minutes). From the top of the hot zone (elevation = 0) to about 6 in. downward into the furnace (elevation = -6), $\Delta T_{ave,sp=900^{\circ}C} \sim 50^{\circ}C$, $\Delta T_{ave,sp=1000^{\circ}C} \sim 90^{\circ}C$, and $\Delta T_{ave,sp=1100^{\circ}C} \sim 140^{\circ}C$ for the three set points tested as shown in Figure 5. In looking at Figure 5, it is evident that the bulk of the hot zone of the furnace was relatively uniform in temperature (especially the region between -2 and -6), except for the regions near the very top (i.e., near 0).

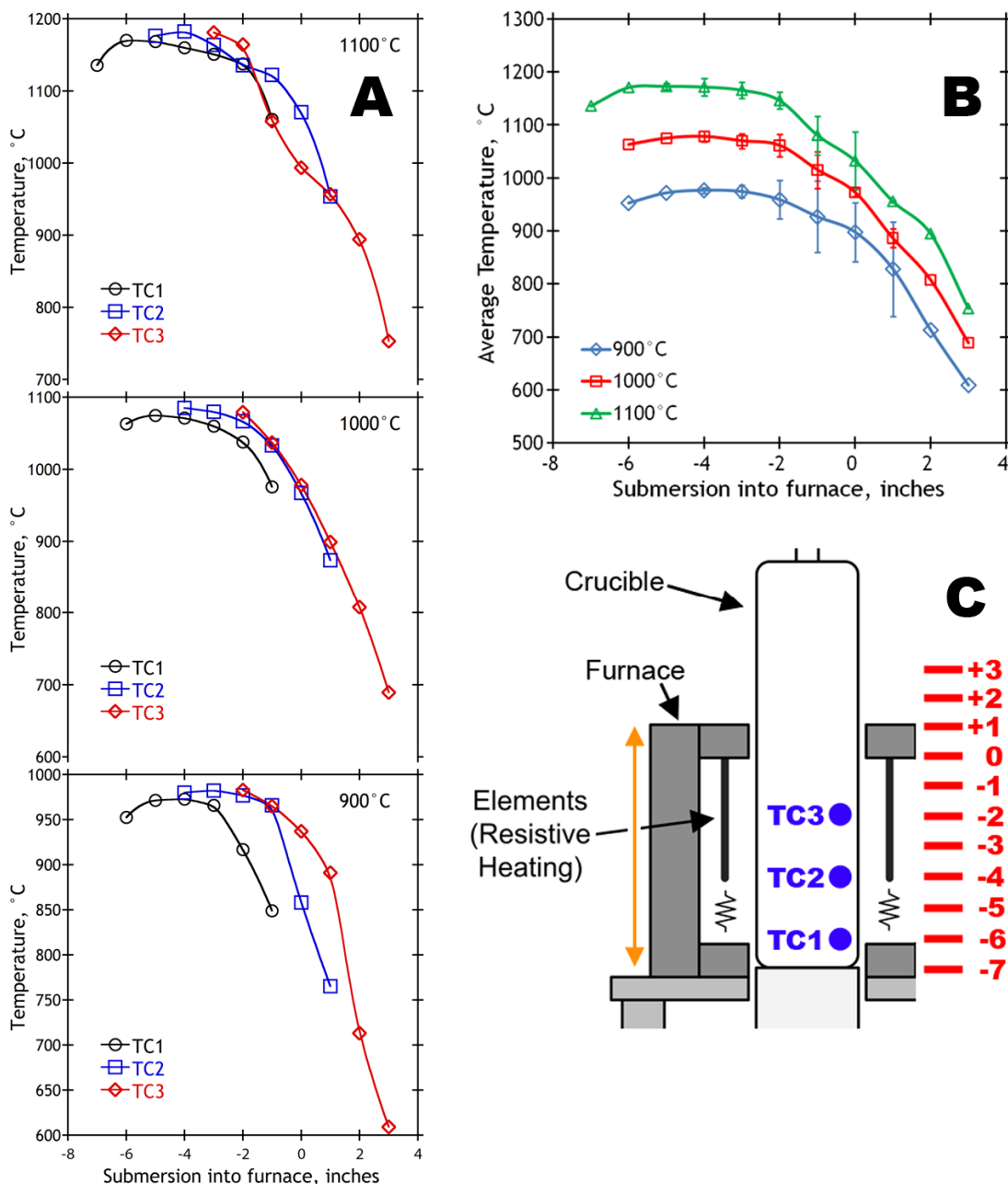


Figure 5. Furnace profiling. (A) The temperature measured by three thermocouples at a distance, *Submersion into furnace*, which was the distance (in inches) from the thermocouple to the top of the hot zone inside the furnace. (B) The summary of average temperature (of all thermocouples) of the different distances with standard deviation where more than one measurement was taken at a given distance. (C) Schematic of the procedure used and how the scale, *Submersion into furnace*, relates to the setup used.

2.4 Melter Run No. 1 (LSM-R1)

Once the melter was operational, the first batch, *LSM-R1*, was prepared (Table 5). At a total of 300 g solids, the resulting mass of glass expected from the complete melt process (i.e., loss of NO_3 , CO_2 , and H_2O) was ~ 215 g. This was batched into a beaker, waste first (with nitrates preceding oxides) followed by the glass formers, and then DIW was added for a total volume of 1 L. The solution was stirred for several hours using a Teflon stir bar on a stir plate.

Table 5. Batch sheet for LSM-R1.

Additive	Mass of additive, g
Ba(NO ₃) ₂	5.22
Ce(NO ₃) ₃ *6H ₂ O	11.39
CsNO ₃	5.52
Eu(NO ₃) ₃ *6H ₂ O	0.60
Gd(NO ₃) ₃ *5H ₂ O	0.54
La(NO ₃) ₃ *6H ₂ O	5.84
MoO ₃	5.42
Nd(NO ₃) ₃ *6H ₂ O	18.96
Pr(NO ₃) ₃ *6H ₂ O	5.30
RbNO ₃	0.93
Sm(NO ₃) ₃ *6H ₂ O	3.81
Sr(NO ₃) ₂	2.78
Y(NO ₃) ₃ *6H ₂ O	2.96
ZrO(NO ₃) ₂ *2H ₂ O	8.98
Al ₂ O ₃	12.91
H ₃ BO ₃	19.26
CaCO ₃	27.10
Li ₂ CO ₃	21.53
Na ₂ CO ₃	25.96
SiO ₂	114.99
Total:	300.00

The beaker of the solution was placed on a stir plate next to the melter and the Tygon[®] feed tube, threaded through the peristaltic pump, was placed into the beaker. The furnace was set to 1200°C with ~1 in. of the crucible inside the hot zone of the furnace. An initial feed rate of ~9 mL/min was used and was increased as the run progressed. As the melting progressed, the furnace was raised to bring more of the crucible into the hot zone as the melting progressed to maintain the melt in the hot zone.

Operational problems during this first run then began to appear. Once 500 mL of the feed (~50% of the volume) was fed to the melter (which took a total of ~120 minutes), the feed line clogged because new feed was not added to the Feed Tank in time and the Tank ran dry. Once the Tank was refilled with new feed, the nozzle became unclogged, and the lines were immediately flushed with DIW to reduce feed build-up inside the line. However, at that point it was apparent that the crucible had broken, and the furnace set point was changed to 500°C in order to quickly cool the glass to $\sim T_g$ and allow it to anneal. Within about 15 minutes, the glass started to make cracking sounds, and it was apparent the crucible was further breaking at which point, the furnace was set up to cool to room temperature, and the annealing step was terminated. The following day, after the system had cooled down to room temperature, the crucible and resulting glass were removed from the furnace. A small cold cap remained on the melt surface. The chunks of glass were assembled using resin to reconstruct the melt in progress. Optical micrographs were collected at different stages of the assembly (Figure 6-A) in order to present the bubbles inside the cold cap as well as the fully assembled piece (Figure 6-B).

The condensates were collected from the inside surfaces of the quartz tube feed and off-gas lines (Figure 9, #1 and #2, respectively) and analyzed using XRD (see Figure 10 and Figure 11), SEM (see Figure 14), and EDS (see Table 11) for crystal structure, appearance, and composition, respectively.

2.5 Melter Run No. 1 (LSM-R2)

The second run, LSM-R2, was done in a similar fashion as LSM-R1 using the same feed composition. The feed used included the volume remaining from LSM-R1 in addition to 1 L of new feed totaling 1280 mL of total feed. The flow rate varied but was ~16 mL/min on average and 22 mL/min at the end of the test. Melting operation was performed for 81 minutes until the furnace was set to anneal at 500°C. The furnace was allowed to cool to 500°C, where the glass was annealed for 2 hours before cooling slowly to room temperature. Upon completion of LSM-R2, the scrubber solutions were collected and placed in Nalgene® bottles.

Optical micrographs were captured of the glass demonstrating the complete vitrification of the feed (Figure 7). Solid condensates from two different regions (the scrubber off-gas line and the Teflon® tube off the crucible; see regions #3 and #4 in Figure 9) were collected and subjected to XRD (Figure 12 and Figure 13), SEM (Figure 15), and EDS (Table 12).

2.6 X-ray Diffraction

XRD was performed on all of the solid condensates collected from both LSM-R1 and LSM-R2 (see section 3.5 Off-Gas Condensate Solids Analysis). The condensates were suspended in a liquid (i.e., ethanol) and a pipette was used to apply a drop or so of the suspension to a fused quartz slide. The slides containing the specimens were then dried in an oven at 60°C for 1 hour, leaving the solids adhered to the slide. The specimens were then analyzed using a Scintag PAD V diffractometer with Cu K α radiation ($\lambda = 1.5406 \text{ \AA}$) at 45 kV and 40 mA and a Peltier-cooled Si(Li) solid state detector. The experiments were done using $\theta/2\theta$ geometry in a step-scan approach from 5°–70° 2 θ with a step size of 0.02° 2 θ and a dwell time of 2 seconds per step. Jade 6® software was used to process and identify phase assemblages. Data were fit initially using a chemistry filter including the batched components, and when peaks could not be fit using the chemistry filter, data were fit without elemental discrimination. In some cases, peak identification was not possible. XRD data was especially critical for detection of possible Li- and/or B-containing phases, which were not identifiable through EDS.

2.7 Scanning Electron Microscopy

SEM and EDS were performed on a randomly selected chunk of glass from LSM-R2 in order to verify the composition for comparison to the target composition. The SEM used was a JEOL 5900 with an EDAX EDS system using a Li-drifted Si X-ray detector. EDS was collected using a 20 KV acceleration voltage, and a collection time of ~10 minutes at ~8,000 counts per minute. SEM/EDS was also performed on two condensates from LSM-R1 (Figure 9, #1 and #2) and two condensates from LSM-R2 (Figure 9, #3 and #4); these were the samples mentioned above which were prepared/analyzed for XRD.

3. RESULTS AND DISCUSSION

3.1 Analysis of Denitration Solution and Precipitates

The three aliquots removed over the course of the thermochemical denitration scoping test were analyzed for NO₃⁻ concentration by ion chromatography as shown in Table 6. Note: the final sample taken was not analyzed intact as the sample container had leaked due to gas pressurization that evolved following the test. The final sample analyzed was removed from the solution that had cooled and was open to the atmosphere for 6 days. The solution was clear with a thick white precipitate at the bottom of the beaker.

Table 6. Ion chromatography of solution aliquots.

Aliquot	NO ₃ ⁻ , mg/L
Prior to test	929,930
After first day, at room temperature	857,797
Final solution, cooled 6 days	774,405

The NO₃⁻ analysis indicated that the concentration of NO₃⁻ remained high throughout the test. Water evaporation and denitration remained steady through the process, although NO₃⁻ did somewhat decrease. As the solution volume decreased, the solids loading in the beaker increased, which also reduced the ionic nitrate concentration.

The vacuum-filtered white precipitate was found by SEM/EDS to be composed of highly oxidized (i.e., NO₃⁻) Mo, Zr, and Ba (>93 atomic%) but the rinsed precipitate was found to be composed only of oxidized Mo (>95 atomic%). Therefore, it was thought that neutral-pH-soluble Zr and Ba nitrates had been dissolved and removed during the DIW rinsing step, leaving behind insoluble Mo and a small amount of Zr. XRD data was not collected on these specimens (see Table 7 for the EDS results).

Table 7. SEM/EDS on thermochemical reduction precipitate before (Unrinsed) and after rinsing (DIW-Rinsed) with DIW to remove compounds soluble in neutral pH.

Precipitate	O	Na	Rb	Sr	Zr	Mo	Cs	Ba	Ce	Nd	Pm	Sm
Unrinsed	43.40	0.75	0.69	2.54	15.06	27.21	0.47	7.55	0.38	1.10	0.40	0.47
DIW-Rinsed	38.72	0.38	0.53	0.48	2.18	56.77	0.13	0.24	0.13	0.08	0.16	0.20

3.2 General Results from Melter Runs

Table 8 shows a comparison between the two LSM runs. General observations made during and after the melter runs include:

- the cold cap did not occupy more than 50% of the melt surface, and the slurry pool covered between 1.75-2 in. in diameter.
- gas generation was observed below the cold cap, which intensified during the cold cap burn-off at the end of the test.
- NO_x generation was observed by the presence of a brown gas inside of the headspace in the submerged bed scrubber; it appeared light brown initially, turned dark brown, and then turned clear until the termination of the feed where it returned to a dark reddish brown.
- white and yellow condensates were present throughout the off-gas lines; this was observed mostly near the crucible, but small quantities were seen even in the line into the submerged bed scrubber, as well as the bath itself.
- the submerged bed scrubber contained 1320 g of additional mass (mostly NO₃) equating to ~660 g/L of feed, the pH of the solution was ~1, and the small quantity of solids collected in the scrubber were yellow, a color that was observed throughout the off-gas lines.

Table 8. General parameters for LSM runs.

Parameter	LSM-R1	LSM-R2
Feed concentration, g/L feed	300	300
Feed rate(s), mL/min	9–16	12–22

Parameter	LSM-R1	LSM-R2
Feed quantity, L	0.5	1.3
Processing time ⁽¹⁾ , min	120	81
Maximum cold cap height, in.	1	1
Cold cap diameter, in.	1.75–2	1.75–2
Mass of glass, g	150	380
Annealed at 500°C	No	Yes
Estimated cold cap recovered, g	20	0

(1) Does not include annealing

3.3 LSM-R1 Results

Pieces of the glass were removed and glued together; pictures were taken of the glass during the assembly process (see Figure 6). The dried, unvitriified feed on top of the glass (cold cap) can be seen in Figure 6 as a white crust.

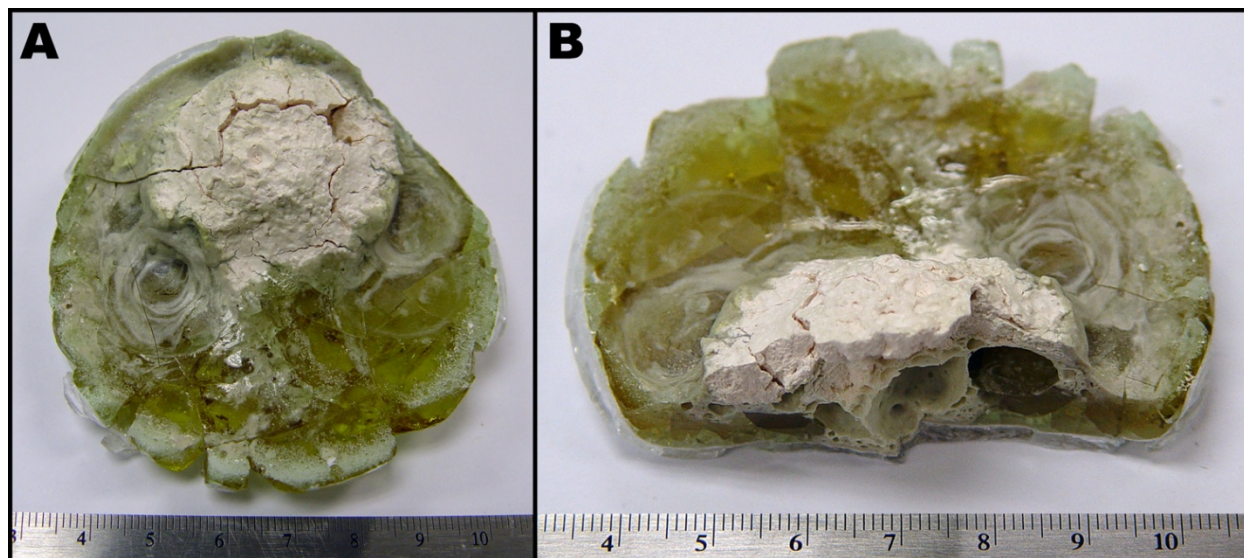


Figure 6. Pictures of LSM-R1 at different stages during assembly of the resultant vitrified feed.

3.4 LSM-R2 Results

Though the quartz tube broke, the break occurred toward the end of the process. The resulting glass was nearly completely homogeneous in appearance. Figure 7-A shows the more homogeneous top portion of the glass. Some of the vitrified feed reacted with the zirconia support following crucible failure – see the white material in Figure 7-B – making exact quantification of the amount of vitrified feed difficult. The quantity was estimated at ~380 g.

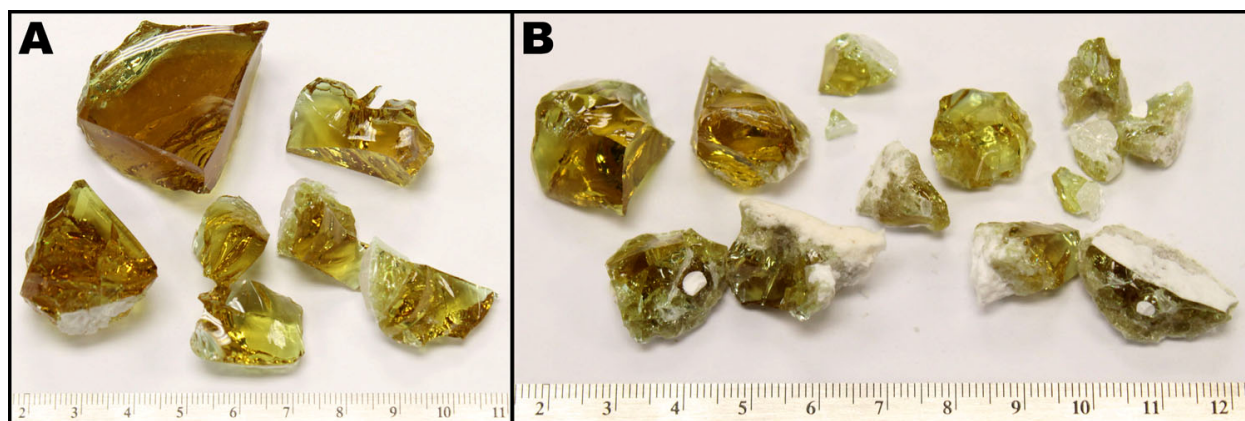


Figure 7. Optical micrographs of the glass produced from LSM-R2. (A) Shows the glass out of the crucible. (B) Shows the glass that stuck to the bottom of the crucible and the zirconia stage.

EDS was captured on a small chunk of bulk glass from LSM-R2 using a high count rate and a long collection time (see section 2.7, Scanning Electron Microscopy). An attempt was made to perform a rough mass balance following LSM-R2 by analyzing the composition of the glass and the condensates (the precipitates in the scrubber bath and the soluble species in the scrubber solutions were not analyzed). Since the crucible broke and species might have evolved from the crucible at that point, mass balance analyses were speculative. However, it is reasonable to assume that whatever chemicals in the feed that were not present in the glass or in the rest of the system (e.g., see Figure 9) were likely dissolved in the scrubber solution as soluble salts (i.e., nitrates). The discussion below focuses on the fate of certain moderately volatile species in the melt, particularly Mo and Cs.

Since EDS is increasingly insensitive to elements with a lower atomic number than carbon, Li and B could not be included in the comparison. The targeted compositions were renormalized with Li and B removed and the targeted compositions were then compared against the values measured using EDS. The comparison is seen in Table 9 with a graphical representation presented in Figure 8. The discrepancies with the SiO_2 (7.6% inflated in measured) and Al_2O_3 (24% inflated in measured) are possibly due to the volatility of other components in the feed which would tend to inflate the Si and Al values, which is consistent with the higher percentages observed for these elements in the measured composition versus the target.

The % difference values for those materials can be attributed to volatility of these components through the off-gas system. The remaining discrepancies can most likely be attributed to the presence of soluble species in the scrubber solution, noting that the scrubber solution analysis for the presence of soluble species is not complete.

Table 9. Differences between the targeted and measured (EDS) compositions for LSM-R2 vitrified feed. “% Diff.” is the % difference between the measured and targeted values.

Oxide	Targeted	EDS	% Diff.
SiO_2	53.45	57.54	7.6%
Na_2O	7.06	6.78	-4.0%
CaO	7.06	6.27	-11%
Al_2O_3	6.02	7.44	24%
Nd_2O_3	3.38	3.28	-3.0%
MoO_3	2.53	1.72	-32%
Ce_2O_3	2.01	1.80	-10%

Oxide	Targeted	EDS	% Diff.
ZrO ₂	1.92	1.19	-38%
Cs ₂ O	1.86	1.73	-7.0%
BaO	1.43	1.33	-7.3%
La ₂ O ₃	1.02	1.02	-0.21%
Pr ₂ O ₃	0.93	0.80	-14%

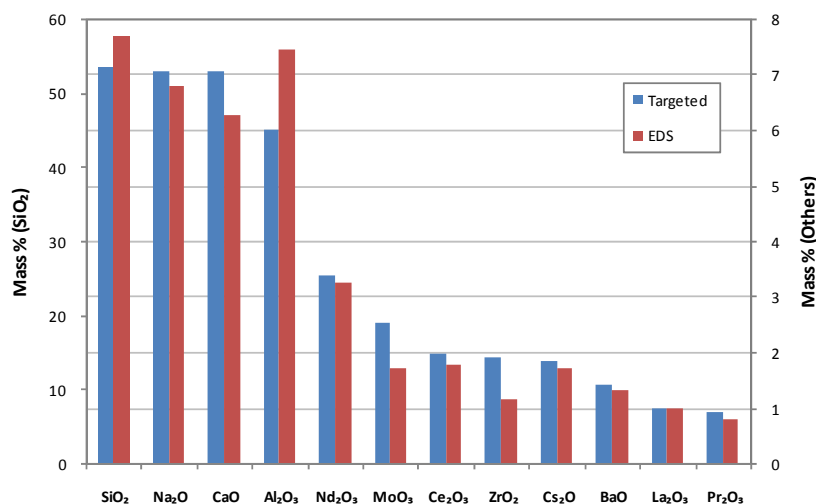


Figure 8. Comparison of targeted and EDS (measured) compositions for vitrified feed from LSM-R2.

3.5 Off-Gas Condensate Solids Analysis

As seen in Figure 9, condensates were removed from the LSM-R1 crucible inlet (#1), the LSM-R1 crucible off-gas (#2), the scrubber feed tube (#3) following LSM-R2, and from the Teflon tube just off the off-gas port on the crucible (#4) following LSM-R2. The colors of the condensates from the crucible feed (#1), crucible off-gas (#2), scrubber feed (#3), and Teflon tubes (#4) were off-white, light tan, light-green/yellow and white/pink, respectively. The appearances of these condensates suggest that the condensate observed on the fused quartz feed inlet port (#1) is the same composition as that seen along the walls of the crucible; it is thought to be feed that splattered on the walls of the quartz tube upon exit from the feed line.

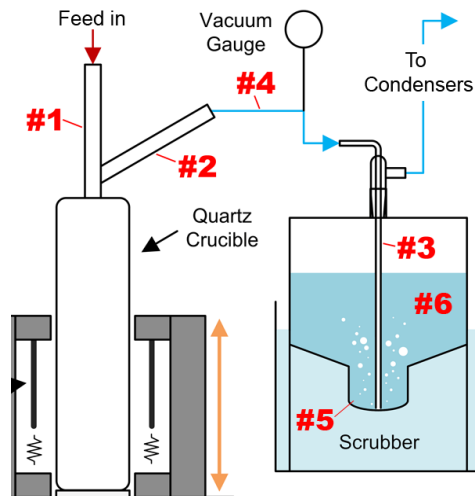


Figure 9. Regions where condensates were observed (#1–#5) and the scrubber solution (#6) where soluble salts were expected. *NOTE: this is a cut-out from Figure 3.*

The powders were recovered by scraping with a metal spatula and were placed in a 50 mL conical centrifuge tube along with the ethanol that was used to aid in removal of the condensates. Condensate-ethanol slurries were centrifuged in order to pelletize the condensate. The liquid then was evaporated by placing the vials in an oven at 60°C overnight. Dry masses were found to be ~2.11 g (of total present, not collected) (Table 10) for all condensates. Not all of the condensates were collected due to accessibility difficulties in the narrow tubes.

Table 10. Quantities (g) of condensates (#1–#4), precipitates (#5), or solutions (#6) collected and estimated for each region from Figure 9. *NOTE: the value for #6 is in mass (g) of the liquid collected from the scrubber solution and since the amount of dissolved materials were never quantified it was not included in the “Totals” value.*

#	Collected, g	Estimated Remainder, g
1	0.4446	0.60
2	0.0516	0.070
3	0.1760	0.35
4	0.0716	0.09
5	-	1.0
6	-	2200
Totals:	0.7438	2.11

Once mass data was collected on the powders, they were re-suspended in ethanol and droppered onto a fused silica slide for XRD, SEM, and EDS. All solid condensates showed a primary phase of quartz (PDF#85-0795) most likely caused by crystallization and spallation of the crucible but may also be caused by feed dusting since it was the most abundant of the feed additives. The XRD data for the inlet (Figure 9, #1) and off-gas (Figure 9, #2) port of the quartz crucible are found in Figure 10 and Figure 11, respectively. The best fit for the diffraction peaks found in the inlet tube (#1) was sodium nitrate (NaNO₃, PDF#79-2056). This seemed to match nearly all of the peaks aside from a few very minor ones. The minor phases detected include: powellite (CaMoO₄, PDF#29-0351), corundum (Al₂O₃, PDF#63-0649), and calcite (CaCO₃, PDF#60-7297).

The best fit for the diffraction peaks found in the off-gas line (#2) included several phases, the fused silica background being the most prominent. The second most abundant phase was sodium nitrate (NaNO_3 , PDF#79-2056) followed by several minor phases including keatite (SiO_2 , PDF#76-0912), aluminum oxide (Al_2O_3 , PDF#78-2427), sodium lanthanum molybdate ($\text{Na}_{0.5}\text{La}_{0.5}\text{MoO}_4$, PDF#63-3549), sodium molybdenum oxide ($\text{Na}_{0.9}\text{Mo}_2\text{O}_4$, PDF#39-1089), powellite (CaMoO_4 , PDF#29-0351), dibarium calcium molybdate ($\text{Ba}_2\text{CaMoO}_6$, PDF#62-5057), sassolite (H_3BO_3 , PDF#61-0209), and molybdenum oxide (Mo_9O_{26} , PDF#65-6343). These fits were based on structure; the actual compositions of the minerals could be a bit different than these ideal formulas.

The XRD results for the condensate in the scrubber feed tube (Figure 9, #3) show the structure of the following phases: corundum (Al_2O_3 , PDF#63-0649), calcite (CaCO_3 , PDF#60-7297), powellite (CaMoO_4 , PDF#60-9226), and dibarium calcium molybdate ($\text{Ba}_2\text{Ca}(\text{MoO}_6)$, PDF#62-5057).

The XRD results for the condensate in the Teflon tube (Figure 9, #4) show the structure of the following: sodium nitrate (NaNO_3 , PDF#79-2056), powellite (CaMoO_4 , PDF#29-0351), cesium nitrate (CsNO_3 , PDF#63-0733), and barium cerate(IV) (BaCeO_3 , PDF#64-3634).

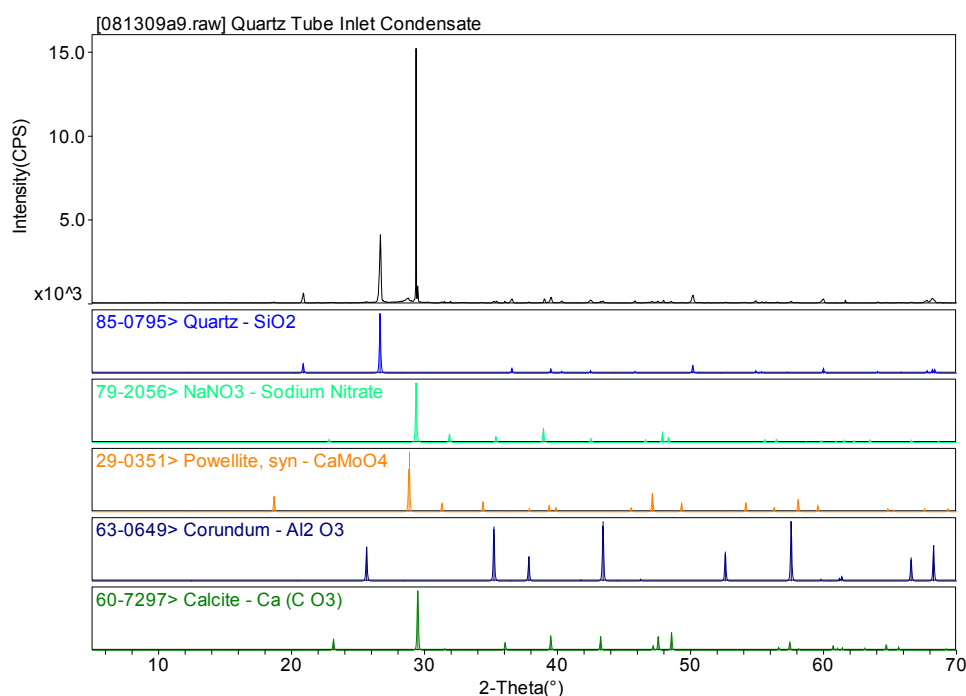


Figure 10. XRD results for the condensate inside the quartz tube inlet from LSM-R1 (Figure 9, #1).

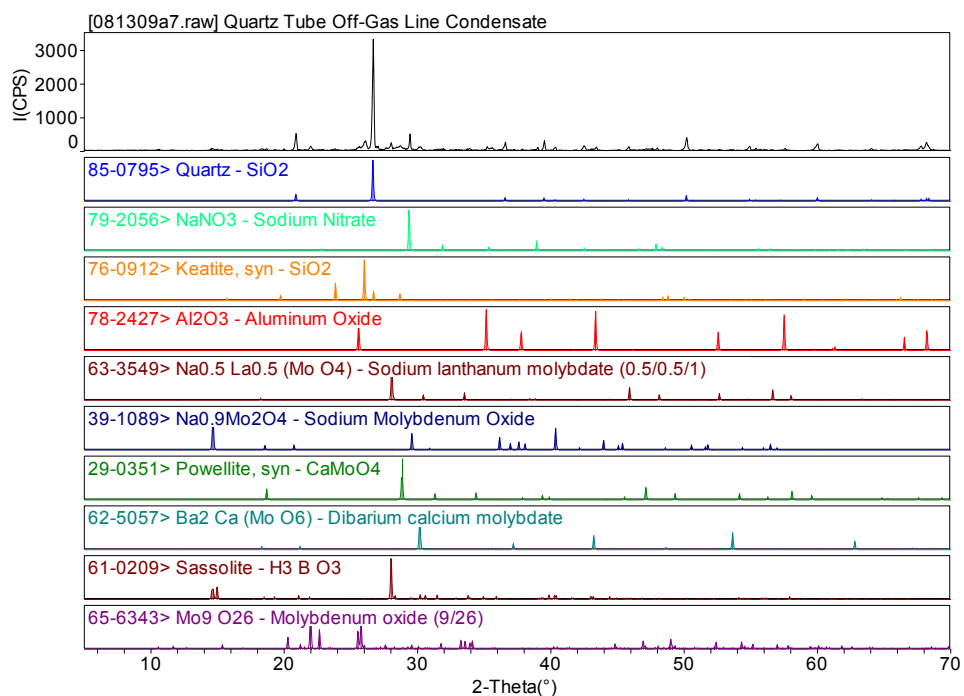


Figure 11. XRD results for the condensate inside the quartz tube off-gas line from LSM-R1 (Figure 9, #2).

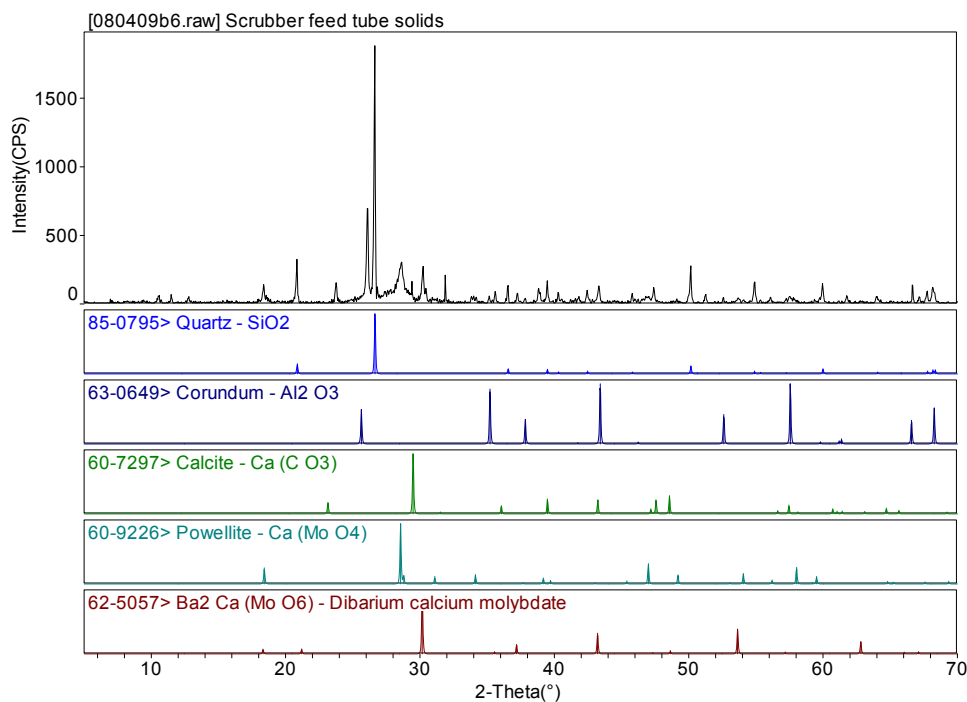


Figure 12. XRD results for the condensate inside the scrubber feed tube from LSM-R2 (Figure 9, #3).

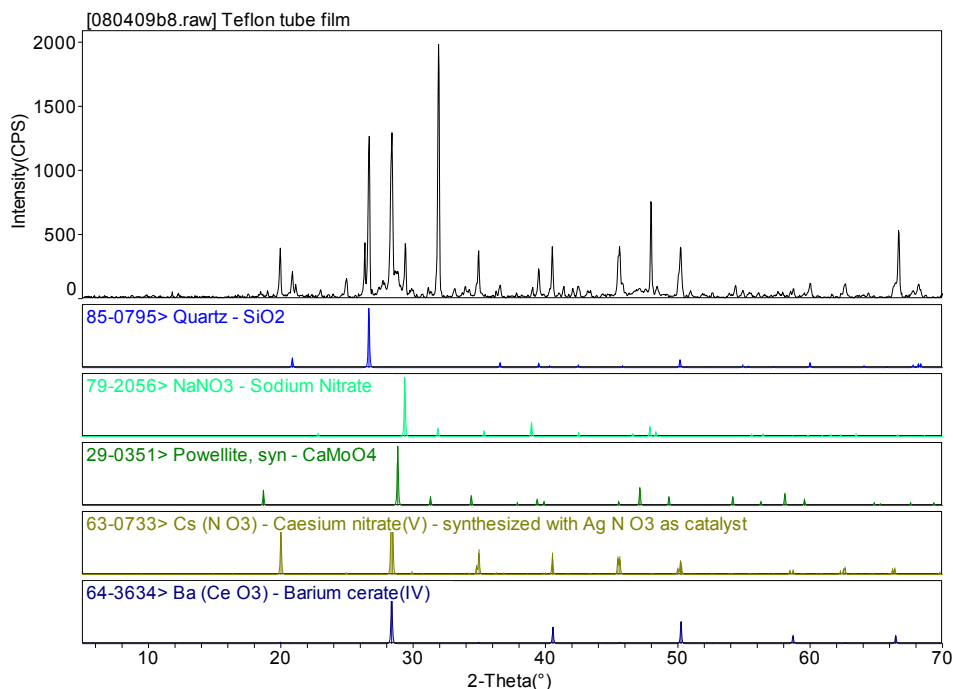


Figure 13. XRD results for the condensate inside the Teflon from LSM-R2 (Figure 9, #4).

The SEM micrographs taken of (A is from Figure 9, #1) and (B is from Figure 9, #2), Figure 14, show microstructure of particles on the order of 50 μm to $<1 \mu\text{m}$. Compositional analysis was taken of low magnification (85 \times) regions of each condensate using EDS, and these results are presented in Table 11. Some of the SiO₂ detected by EDS could be noise contributed by the quartz substrate. Disregarding the inflated values for Si due to the added signal from the substrate, the high oxygen levels – which are under-compensated by the EDS detection system by $\sim 42\%$ as determined by calibration – allude to the presence of a nitrate. Several different cations were detected in both specimens suggesting the presence of a mixture of various nitrates in both solutions. The off-gas line had higher quantities of the volatiles than the inlet line, i.e., Mo (2.7 \times) and Cs (2.3 \times), and lower quantities of others, i.e., Ca, Ce.

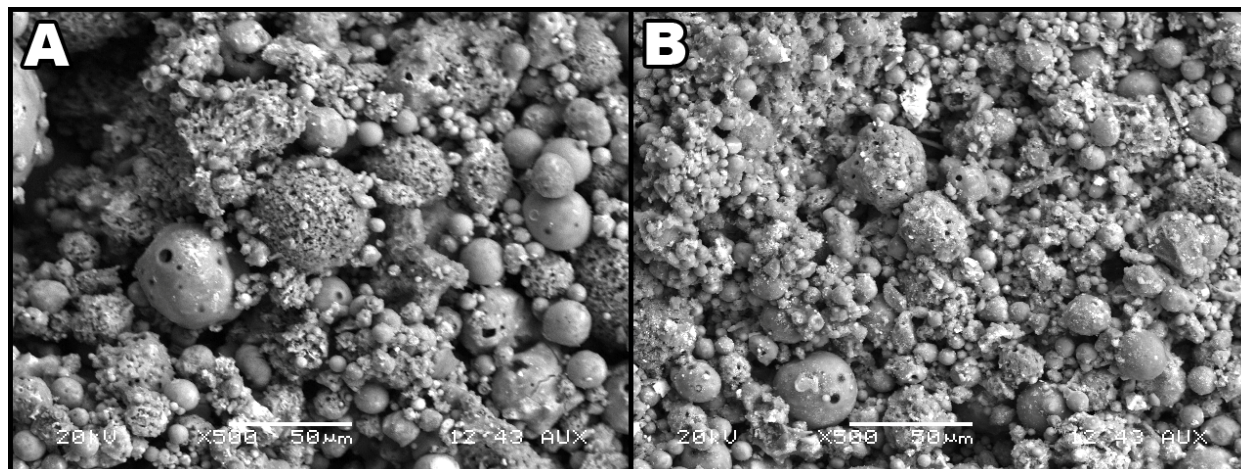


Figure 14. (A) SEM on the condensates collected off the inside of the inlet port on the quartz crucible (Figure 9, #1) at 500 \times and (B) SEM on the condensates from the off-gas line on the quartz crucible (Figure 9, #2) at 500 \times .

Table 11. EDS results (in mass%) from LSM-R1 crucible condensates listed by element. “Inlet” and “Off-Gas” correspond to #1 and #2, respectively from Figure 9.

#	Specimen	O	Na	Al	Si	Zr	Mo	Ca	Cs	Ba	La	Ce	Nd
1	LSM-R1, Inlet	35.52	4.53	3.76	38.36	1.30	3.17	4.46	3.22	1.15	0.73	1.46	2.34
2	LSM-R1, Off-Gas	30.10	4.07	4.16	36.83	1.57	8.64	2.29	7.28	1.36	0.66	0.00	3.03

The SEM micrographs in Figure 15 showing condensates from the scrubber feed tube (A is from Figure 9, #3) and the Teflon tube (B and C are from Figure 9, #4) look slightly different from those showing condensates removed from the crucible as previously described. Both contain dark particles and much brighter particles. The scrubber feed tube condensate appears to be lightly “dusted” with bright particles, with the average particle size <math><1-5\ \mu\text{m}</math>, and in the Teflon tube condensate, the bright particles appear large and faceted, and, are $\sim 20-30\ \mu\text{m}$ on the elongated axis (see “1” in Figure 15-C). The different types of particles from the Teflon tube condensate can be seen in the higher magnification micrograph in Figure 15-C. Spot EDS analysis was performed on the three regions denoted by boxes in Figure 15-C, and the following characterization information was obtained:

1. elongated, faceted particle with high average atomic number (by the brightness under backscattered SEM); the composition appears to be mostly composed of Cs-O (~ 80 mass%).
2. densely packed fibrous material; the composition was very high in Mo, Cs, Na, and O (composed ~ 95 mass%).
3. spherical particles; mostly composed of Si-O (~ 75 mass%) with moderate quantities of Na (6.9 mass%), Al (5.7 mass%), rare earths (6.7 mass% Nd, 3.2 mass% Pr), and small quantities of Mo (2.3 mass%) and Cs (3.0 mass%). Note: Particle size distribution and morphology for the SiO_2 particles in the feed versus the condensates were never investigated for comparison.

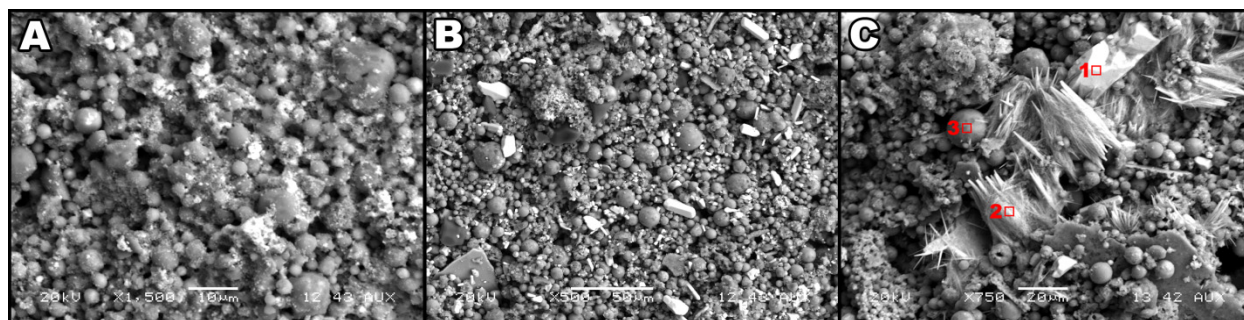


Figure 15. (A) SEM micrograph ($1.5\ \text{k}\times$) of scrubber feed line condensate collected at end of LSM-R2 (#3, Figure 9), (B) SEM micrograph ($500\times$) of the condensate inside of the Teflon tube from LSM-R2 (#4, Figure 9), and (C) SEM micrograph ($750\times$) of Teflon tube condensate (#4, Figure 9). The boxes and labels in (C) show the locations of small area EDS analysis that was performed.

The EDS analysis for $85\times$ fields of view of both condensates (Table 12) shows similar compositions. Both the scrubber line and Teflon line condensates showed high concentrations (in mass%) of the volatile elements Mo ($\sim 10, 12\%$) and Cs ($\sim 12, 16\%$), and exhibited moderate quantities of Na ($\sim 3, 4\%$), Al (3, 3%), Ca (1, 4%), and Nd (2, 3%). It is interesting to note that even though the overall chemistry was similar between these two condensates, not only were their appearances different but, according to the XRD results, the structures seem to be different as well.

Table 12. EDS results (in mass%) from LSM-R2 condensates listed as element.

Specimen	O	F	Na	Al	Si	Zr	Mo	Cl	Ca	Cs	Ba	La	Nd
LSM-R2, Scrubber	29.67	1.01	3.43	2.92	34.53	1.38	10.01	0.09	1.14	12.41	1.07	0.11	2.23
LSM-R2, Teflon	24.99	2.46	4.45	3.19	26.24	1.25	11.75	0.37	3.80	16.27	1.20	0.80	3.23

In comparison of the elemental distribution across the four condensates analyzed, as seen by a column chart in Figure 16 (balance is SiO₂), it is evident that the volatile compounds (i.e., Cs, Mo) were carried out of the crucible, into the off-gas line, and largely concentrated in the Teflon tube (Figure 9, #4). Of the other compounds observed in the condensates, some were observed at highest concentrations nearest the crucible and others seemed to be present at similar concentrations throughout the condensate paths (i.e., Al₂O₃).

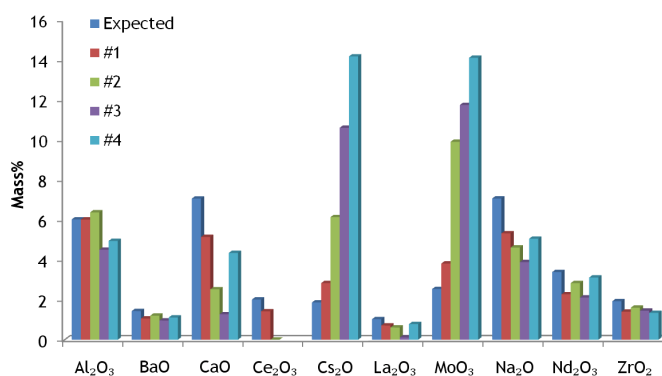


Figure 16. Quantities (in mass%) of each additive (except for SiO₂) in condensates #1–#4 (see Figure 9).

4. CONCLUSIONS AND FUTURE WORK

The highlights of this study include:

- Some methods are proposed to concentrate the solids (i.e., thermochemical reduction, HNO₃ distillation) due to the very low concentrations of solids in the waste stream.
- Two melter runs were completed using a feed based on the composition of the baseline glass limited by high MoO₃, CSLNTM-C-2.5 (without noble metals and minor components).
- Small quantities of solid condensates were observed in the off-gas system through both experiments (in both the inlet and off-gas ports of the crucible) as well as the Teflon tube and scrubber feed tube in the off-gas line.
- Condensates were high in alkali (Na, Cs), alkaline earth (Ca, Ba), Mo, and Al; several nitrates and carbonates were also observed.

Some soluble off-gas compounds (nitrate salts) are expected to have dissolved into the scrubber solution. However, funding and time did not permit analysis of the scrubber solution to verify. The composition of the glass obtained through the second melter run was close to the target composition except for three components: Al, Mo, and Zr. Due to structural failures in both melter runs, it was determined that a new crucible design would be required for future runs. A new crucible has been designed and fabricated that will be used for future runs if funding permits.

Future work will include additional melter runs with acidic feed (i.e., 3 M HNO₃). The scrubber solution should be analyzed for soluble compounds, and the precipitate at the bottom of the scrubber bath should be analyzed for composition. The system could be further designed to meet off-gas requirements, i.e., a

recuperator should be designed and included in the system to recycle the off-gas condensates back into the melter. Upon determination of a successful melter configuration, scaled-up experiments should be performed. Finally, the management of heat generated by Cs/Sr decay will have to be evaluated.

5. ACKNOWLEDGEMENTS

Authors would like to thank the U.S. Department of Energy, Office of Nuclear Energy (DOE-NE), for their support of this work under Contract Number: DE-AC05-76RL01830. Authors thank Joe Ryan and Loni Peurrung for helpful review of this document, Sue Lesica (DOE-NE) and Terry Todd (Idaho National Laboratory) for project oversight, and Jim Buelt and Loni Peurrung for PNNL management of this AFCI activity.

6. REFERENCES

- Benker, DE, LK Felker, ED Collins, PD Bailey, JL Binder. 2008. *Testing of Chemical Separation Flowsheets for the Global Nuclear Energy Partnership (GNEP)—Results from the First “Coupled End-To-End (CETE) Campaign Using Long-Cooled LWR Fuel*, Oak Ridge National Laboratory, Oak Ridge, Tennessee.
- Bray, LA. 1963. *Denitration of PUREX Wastes with Sugar*. HW-76973, UC-70 Waste Disposal and Processing TID-4500, 27 ed. Hanford Atomic Products Operation, Richland, Washington.
- Crum, JV, AL Billings, J Lang, JC Marra, C Rodriguez, JV Ryan, JD Vienna. 2009. *Baseline Glass Development for Combined Fission Products Waste Streams*, AFCI-WAST-WAST-MI-DV-2009-000075, Pacific Northwest National Laboratory, Richland, Washington.
- Smith, HD, EO Jones, AJ Schmidt, AH Zacher, MD Brown, MR Elmore, SR Gano. 1999. *Denitration of High Nitrate Salts Using Reductants*, PNNL-12144, Pacific Northwest National Laboratory, Richland, Washington.